8TH INTERNATIONAL SYMPOSIUM ON PARTICLE IMAGE VELOCIMETRY - PIV09
Melbourne, Victoria, Australia, August 25-28, 2009

3D3C Velocity Measurements Downstream of Artificial Heart Valves

D. Amatya[1], D. R. Troolin[2] and E. K. Longmire[3]

[1] Department of Biomedical Engineering, University of Minnesota, Minneapolis, MN, USA
amatya@umn.edu

[2]Fluid Mechanics Research Instruments, TSI Incorporated, Shoreview, MN, USA

[3]Department of Aerospace Engineering and Mechanics, University of Minnesota, Minneapolis, MN, USA

ABSTRACT

Three-dimensional three-component (3D3C) velocity measurements were made in the flows surrounding a mechanical valve and a silicone polymer valve. Primary three-dimensional flow features were identified in the instantaneous and ensemble-averaged flows surrounding both valves.

1. INTRODUCTION

Flow through heart valves is inherently complex in that it is both unsteady and three dimensional. A number of studies have examined steady and pulsating flow through mechanical heart valves using planar or stereo PIV [3, 8]. As these techniques determine velocity within planes, data in multiple planes can be combined to give reasonable estimates of averaged flow behavior over a volume. However, instantaneous results are of interest for understanding local variations in velocity, including shear and strain fields, due to the potential effects on blood and endothelial cells. Computational studies of flow through mechanical valves have shown the inherent three-dimensionality in instantaneous fields [1]. However, we are unaware of any *in vitro* studies that capture volumetric flow fields.

The purpose of the present work was to demonstrate the potential of a volumetric 3-component velocimetry (V3V) system to obtain full velocity fields surrounding and downstream of artificial heart valves. Flow through a mechanical valve with steady upstream conditions was examined to validate the experimental technique. Then, we examined pulsating flow through a transparent deformable bileaflet silicone valve of geometry matched to tissue-engineered valves designed to be aortic valve replacements [7, 9].

2. METHODS

A 19 mm St. Jude Medical Regent mechanical valve (MV) shown in Fig. 1(a) housed within an acrylic tube (modelling a rigid aorta) of inner diameter D_T = 25.4 mm was placed in a steady recirculating flow loop. The internal working fluid and fluid external to the tube were indexed matched to that of the acrylic tube (1.49) to minimize optical distortion due to the tube curvature. The working fluid was 60% by weight sodium iodide solution (η = 1.1E-6 m^2/s) operating at 5 L/min with a corresponding tube Reynolds number of 4200. The average velocity U_{MV} based on this Reynolds number and D_T was 0.165 m/s.

A transparent silicone deformable bileaflet valve (SV), shown in Fig. 1(b), with an inner diameter D_{SV} = 20mm was tested in a cardiovascular pulse duplicator. When the valve is undeformed, the two leaflets area 1 mm apart along a slit with length = 20mm. When a positive pressure difference is applied across the valve, the leaflets deform yielding an elliptically shaped opening. The internal working fluid and fluid external to the SV were indexed matched to the SV (1.43). The working fluid for the SV was 40/60% by volume water and glycerin solution (ρ = 1.15 g/cm^3, η ~ 6.58 mPa•s). A 70mL volume of the working fluid was displaced in each cycle at a rate of 70 beats/min by the pulsatile pump resulting in an average flow rate of 4.2L/min. The average velocity U_{SV} based on this flow rate and D_{SV} was 0.22 m/s. Pressure and flow signatures were measured using Vivitro systems pressure transducers and a Carolina Medical electromagnetic flow meter, respectively. Pressure drop measurements were obtained at streamwise locations approximately $\pm 2D_{SV}$ down and upstream of the SV. Flow rates were measured upstream of the SV.

A three-aperture, volumetric 3-component velocimetry (V3V) was used to obtain the 3D3C velocity fields, which is based on the defocusing digital particle image velocimetry (DDPIV) technique first proposed and established by Willert and Gharib [10]. Pereira et al. [5] used a technique based on the original concept but with a three camera setup to map a bubbly flow around a propeller. The technique was further improved and characterized by Pereira et al [4] and Kajitani and Dabiri [2], respectively. The current study uses the technique as described by Pereira et al [5] and a relaxation method of 3D particle tracking as described by Pereira et al. [6], whereby a volumetric velocity field is obtained by identifying 2D particles in six images from three distinct apertures at two separate times, reconstructing the 3D particle locations in space through analysis and comparison to a calibration, tracking the 3D particles from the first image capture to the second, and interpolating the randomly spaced vector cloud onto a rectangular grid.

The flow was illuminated by a dual-head Nd:YAG laser with 50 mJ/pulse as shown in Fig. 2. A combination of two 25mm focal length cylindrical and three 500 mm focal length spherical lenses were mounted in front of the beam exit in perpendicular orientations to produce an ellipsoidal cone of laser light. The three-aperture camera was mounted 625 mm from the measurement region at 90° to the illuminating light. Pairs of laser pulses were separated by 50-1200 μs depending on the instantaneous flow rate, and 42 micron silver-coated hollow glass spheres were identified and tracked in 3D space. The resulting measurement volume was a rectangular prism approximately 28mm × 28mm × 130mm for the 19mm MV ($1.1D_{MV} \times 1.1D_{MV} \times 5.1D_{MV}$) and 18mm × 18mm × 40mm ($0.9D_{SV} \times 0.9D_{SV} \times 2\ D_{SV}$) for the 20mm SV. A typical single capture yielded between 3,000 and 5,000 independent

randomly-spaced velocity vectors for the MV, and between 400-1000 vectors for the SV. The vectors were interpolated onto a rectangular grid using Gaussian-weighted interpolation. The average spatial resolution for the instantaneous velocity fields was approximately 2.5mm.

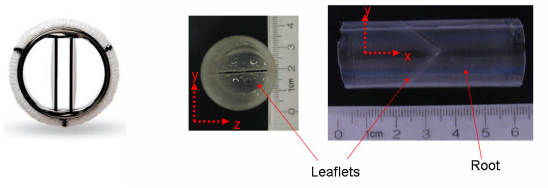

(a) **(b)**

Figure 1. (a) Mechanical valve upstream view and (b) deformable transparent silicone valve downstream and V3V camera views.

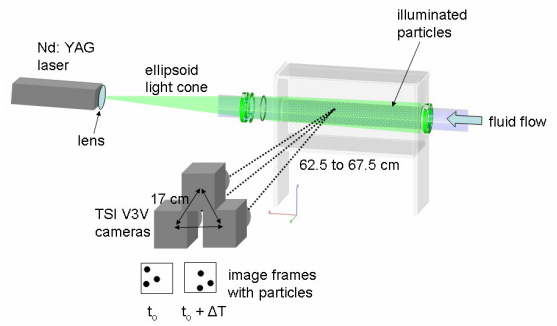

Figure 2. V3V setup.

3. RESULTS

An ensemble-averaged plot of 100 realizations of the flow downstream of the MV can be seen in Fig. 3. The plot in the upper left shows a view looking from the valve downstream. The plot on the right shows the flow moving from left to right, with the valve exit located at $x/D_{MV} = 0$. Slice contours show streamwise velocity, the red isosurface represents streamwise velocity = $1.6U_{MV}$, and the gray isosurface represents streamwise velocity = $0.9U_{MV}$. In general, the 3D3C results compare very well with those captured using planar particle image velocimetry [3]. The red isosurface highlights the presence of three high velocity jets emerging from the valve which correspond to the three openings there. The center jet is oriented directly downstream, while the two side jets have an outward component toward the pipe walls. Further downstream of the valve near $x/D_{MV} = 2$, the center jet begins to dissipate, and the velocity distribution is bimodal. This is consistent with previous PIV findings, but substantially different from the flow pattern observed downstream of a human heart valve, which includes a single high-velocity jet located at the center. Farther downstream near $x/D_{MV} = 3$, the two primary jets merge to form a single jet at the center of the pipe.

Fig. 4 shows the pressure difference across and flow signatures through the SV averaged over ten cycles. The SV is open for approximately one-third of the cycle as indicated by the positive pressure difference and flow rates. The valve is closed for the remaining two-thirds of the cycle as indicated by approximately zero-baseline flow rates and negative pressure differences.

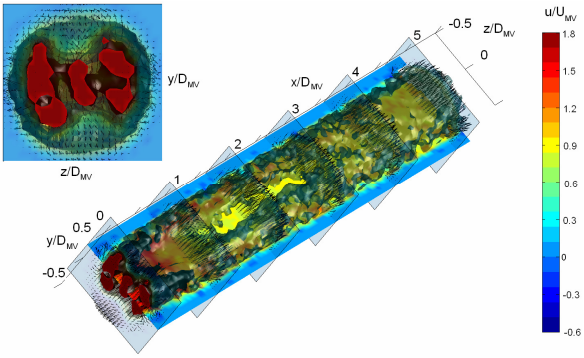

Figure 3. Ensemble-averaged 3D3C plot of the MV. Red isosurface is streamwise velocity at $1.6U_{MV}$ and gray isosurface is streamwise velocity at $0.9U_{MV}$.

3D3C measurements were made for seven phases of the cycle. Flow field measurements and deformation are presented for t = 0.325 and 0.625 s corresponding with open and closed phases of the SV respectively (see Fig. 4). Fig 5(a) shows a raw image of the 'open' phase. The leaflets are bulged outwards towards the downstream end, and the opening dimension is approximately $0.37D_{sv}$ in this view. The root expands beyond the defined Cartesian grid in y at different points along the x axis, and the SV has a 2º downward inclination. Minor ticks of the grid are spaced $0.075D_{sv}$ apart, where velocity vectors are calculated. Also in this image, the particle density through the volume of the SV is shown as seen by one V3V camera. Although particles appear dim near the top and bottom, valid vectors were obtained in those locations.

Fig 5(b) traces out the edges of the valve in green extracted from a raw image. The SV edges are defined as the internal root wall and downstream leaflet surface as identified on the z/D ~ 0 plane. Vectors in the x,y-plane at z/D = 0, along with ω_z contours are depicted. The upstream velocity has a dominant x-component approximately of $5U_{SV}$ with the higher velocities slightly skewed towards y/D = -0.5. The asymmetry is due to an asymmetric inlet condition from the pulse duplicator. The predominantly streamwise velocity vectors turn inwards as they approach the SV leaflets. The vector magnitudes immediately upstream and downstream of the leaflet wall are near zero. A significant amount of ω_z is generated near the upstream leaflet walls before the fluid exits the valve leaflets. The red and blue contours represent clockwise and counter-clockwise rotation respectively. This vorticity in the upstream flow extends into the shear layer downstream where the thickness of the high vorticity zone expands. The flow accelerates through the SV and generates a jet downstream. The vectors along the jet periphery have inward and upstream components almost to the end of the field of view indicating recirculating zones.

The boundary of the valve root and leaflet in the x,z-plane, tracked separately by video data, is overlaid on the velocity vector field with the ω_y contour shown in Fig 5(c). The vectors are fairly uniform in size throughout this field except at the location of the SV leaflet opening. Near x/D = -1.25, the vectors are directed outwards in the z-direction which is

consistent with the local radial extension of the valve root. Velocity vectors do not extend to the walls, since illuminated particles were sparse in those locations, and no particle tracks were generated. For this reason, vectors are not seen on or near the valve walls, so that the no-slip condition is not observed.

Fig. 5(d) shows a different view of the same flow. Two vector fields at y,z-planes of x/D = -0.25 and -1.25 are shown. These vectors are mostly directed in the streamwise direction. An isocontour of streamwise velocity with magnitude of $5U_{SV}$ is plotted in green. The contour shows that the momentum is spread over a wide area upstream of the valve but then is squeezed through the slot-like opening yielding a narrower distribution in both y and z directions that eventually spreads downstream.

Fig. 6(a) shows a raw image of the closed phase of the SV. The root is still larger in diameter than the dimensions of the grid and certain locations along the x-axis. The leaflets seem to reverse in curvature and are now convex with respect to the upstream as compared with the open phase. The intensity of the light is similar to that in 5(a), but the particle number density is larger due to heavier seeding.

Fig. 6(b) shows an x,y plane of vectors at z/D = 0, and the approximate leaflet positions are outlined in green. Once again the root is slightly distended in the radial direction compared to its undeformed state, and the valve is tilted slightly downwards. The velocity vectors are overlaid with ω_z contours. The vectors are much smaller in magnitude as is seen by the $0.5U_{SV}$ reference vector, as compared with $5U_{SV}$ for the open phase. Also, the vorticity is decreased by more than an order of magnitude for the closed phase as compared with the open phase. Clockwise and counter-clockwise rotating structures are present upstream and downstream of the closed leaflet respectively.

Fig 6(c) shows velocity vectors on the x,z-plane at y/D = 0 along with ω_y contours and the deformed state of the SV obtained from the video data. Larger but multidirectional velocity vectors are present upstream and downstream of the SV as compared with the location of the leaflets. Velocity vectors on the y,z-planes at x/D = -0.25 and -1.25 along with an isocontour of 3D swirling strength are shown in Fig. 6(d). The isocontour identifies a large 3D structure rotating upstream of the SV leaflets.

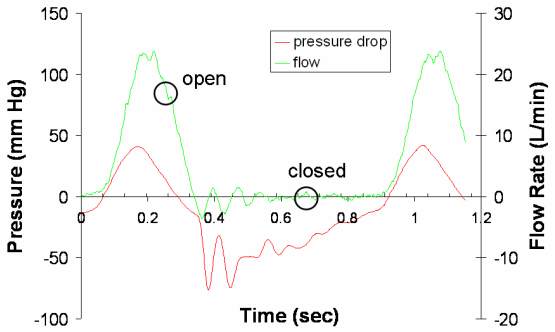

Figure 4. Pressure difference across and flow rates through the silicone valve averaged over 10 cycles. Positive pressure indicates higher upstream pressures and zero mmHg is atmospheric pressure. Circles indicate phases at which 3D3C data is presented for open (t = 0.325 s) and closed (t = 0.625 s) valve states.

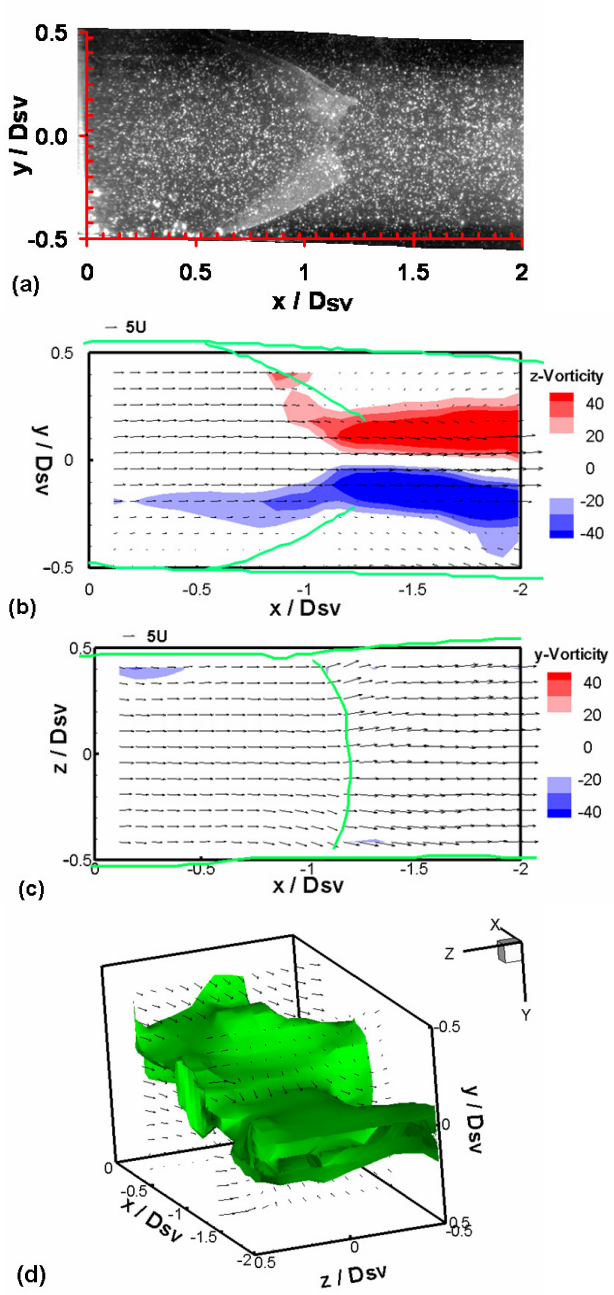

Figure 5. (a) Open phase of SV and illuminated particles as seen by one V3V camera, (b) x-y velocity field with ω_z contour at z/D = 0 plane, (c) x-z velocity field with ω_y contour at y/D = 0 plane, and (d) y-z velocity fields at x/D = -0.25 and -1.25 planes with streamwise velocity isocontour of $5U_{sv}$.

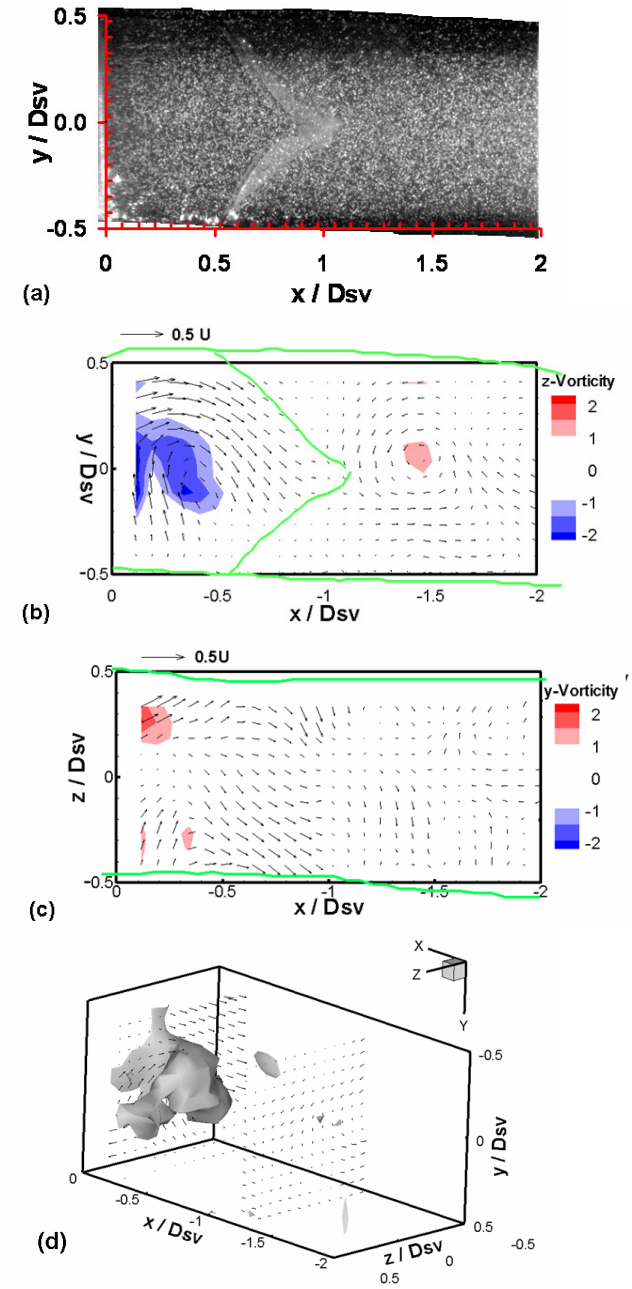

Figure 6. (a) Closed phase of SV and illuminated particles as seen by one V3V camera, (b) x-y velocity field with ω_z contour at z/D = 0 plane, (c) x-z velocity field with ω_y contour at y/D = 0 plane, and (d) y-z velocity fields at x/D = -0.25 and -1.25 planes with normalized swirl isocontour = 0.6.

4. CONCLUSIONS

The V3V technique was used to measure the volumetric velocity fields downstream of a mechanical heart valve and upstream and downstream of a transparent deformable heart valve. Ensemble-averaged results yielded very high spatial resolution (<1mm) data that matched well with that of the literature [3]. Instantaneous velocity fields yielded lower spatial resolution (~2.5mm), but clearly identified the primary features of the unsteady three-dimensional flow.

The 3D3C measurements showed the slot-like elliptical jet flowing through the SV leaflets during the open phase. The elliptical jet is wider along the z-direction than the y-direction corresponding with the bileaflet geometry of the SV. High vorticity levels along the inner surfaces of the leaflets during this phase are indicative of relatively high shear in those locations and the potential for high shear stress on the endothelial wall lining there. Velocities and shear forces are much lower during the closed phase, although recirculation zones were present in both open and closed phases. The strongest vorticity components were aligned with the elongated slit between the undeformed valve leaflets in both open and closed phases.

ACKNOWLEDGMENTS

NIH (NIH/NHLBI 1R01HL071538-01).

REFERENCES

[1] Ge L, Dasi L P, Sotiropoulos F, Yoganathan A P (2008) Characterization of hemodynamic forces induced by mechanical valves: Reynolds vs. viscous stresses. Annals of Biomedical Engineering. 36 #2:276-297.

[2] Kajitani L, Dabiri D (2005) A full three-dimensional characterization of defocusing digital particle image velocimetry. Meas Sci Technol 16:790–804

[3] Marassi M, Castellini P, Pinotti M, Scalise L (2004) Cardiac valve prosthesis flow performances measured by 2D and 3D-stereo particle image velocimetry. Experiments in Fluids 36:176-186.

[4] Pereira F, Gharib M (2002) Defocusing digital particle image velocimetry and the three-dimensional characterization of twophase flows. Meas Sci Technol 13:683–694

[5] Pereira F, Gharib M, Dabiri D, Modarress D (2000) Defocusing digital particle image velocimetry. A 3-component 3-dimensional DPIV measurement technique. Application to bubbly flows. Exp Fluids 29:S78-S84

[6] Pereira F, Stuer H, Graff E C, Gharib M (2006) Two-frame 3D particle tracking. Meas. Sci. Technol. 17:1680-92.

[7] Robinson P S, Johnson S L, Evans M C, Barocas V H, Tranquillo R T (2008) Functional tissue-engineered valves from cell-remodeled fibrin with commissural alignment of cell-produced collagen. Tissue Engineering: Part A14:83-95

[8] Shipkowitz, T, Ambrus J, Kurk J, Wickramasinghe K (2002) Evaluation technique for bileaflet mechanical valves. J. Heart Valve Disease. 11#2:275-282.

[9] Syedain, Z H, Weinberg, J S, Tranquillo, R T (2008) Cyclic distention of fibrin-based tissue constructs: Evidence of adaptation during growth of engineered connective tissue. PNAS 105:6537-6542.

[10] Willert CE, Gharib M (1992) Three-dimensional particle imaging with a single camera. Exp Fluids 12:353–35